Nuclear Engineering and Technology 54 (2022) 554–564

Contents lists available at ScienceDirect

Nuclear Engineering and Technology

journal homepage: www.elsevier.com/locate/net

Original article

Experimental investigation and validation of TASS/SMR-S code for single-phase and two-phase natural circulation tests with SMART-ITL facility

Hwang Bae [a, *], Ji-Han Chun [a], Eunkoo Yun [b], Young-Jong Chung [a], Sung-Won Lim [a], Hyun-Sik Park [a]

[a] Korea Atomic Energy Research Institute, 111 Daedeok-daero, 989 Beon-gil, Yuseong-gu, Daejeon, 34507, Republic of Korea
[b] Eco-friendly Smart Ship Parts Technology Innovation Center, Pusan National University, Busan, 46241, Republic of Korea

ARTICLE INFO

Article history:
Received 1 April 2021
Received in revised form
3 August 2021
Accepted 17 August 2021
Available online 22 August 2021

Keywords:
Single-phase natural circulation
Two-phase natural circulation
SMART-ITL
TASS/SMR-S code

ABSTRACT

The natural circulation phenomena occurring in fully integrated nuclear reactors are associated with a unique formation mechanism. The phenomenon results from a structural feature of these reactors involving upward flow from the core, located in the central-bottom region of a single vessel, and downward flow to the steam generator in the annulus region. In this study, to understand the natural circulation in a single vessel involving a multi-layered flow path, single-phase and two-phase natural circulation tests were performed using the SMART-ITL facility, and validation analysis of the TASS/SMR-S code was performed by comparing the corresponding test results. Three single-phase natural circulation tests were sequentially conducted at 15%, 10%, and 5% of full-scaled core-power without RCP operation, following which a two-phase natural circulation test was successively conducted with an artificial discharge of coolant inventory. The simulation capability of the TASS/SMR-S code with respect to the natural circulation phenomena was validated against the test results, and somewhat conservative but reasonably comparative results in terms of overall thermalhydraulic behavior were shown.

1. Introduction

The natural circulation (NC) behavior of reactor coolant systems (RCSs) plays a significant role in reducing the thermal energy during the transient situation with the reactor coolant pump (RCP) trip, and it is generally driven by the buoyancy and gravity between the heat source and sink [1]. The NC phenomenon in an integral-type reactor is associated with a unique formation mechanism owing to a structural feature of the reactor, involving upward flow from the core located in the bottom region of a single vessel and downward flow to the steam generator in the annulus region. International needs for nuclear safety improvements following the Fukushima Daiichi nuclear power plant accident have accelerated the development of passive safety systems, and new passive safety features have been implemented in the most advanced integral reactors. It is expected that the NC characteristics will have an important influence over the performance of passive safety systems.

Previous investigations on NC phenomena focused on flow regimes and maps based on the experimental results of six pressurized water reactor (PWR) simulators: Semiscale Mod2A, LOBI Mod2, SPES, PKL-III, BETHSY, and LSTF [2]. The investigation of primary single-phase NC in system-integrated modular advanced reactors (SMARTs) using a reduced-height integral test loop (VISTA) has been reported [3]. A generalized correlation has also been proposed to estimate the steady flow rate in two-phase NC loops [4].

The SMART is a small-sized integral reactor with a thermal power of 365 MW, developed by the Korea Atomic Energy Research Institute (KAERI) to supply both power and desalinated seawater [5,6]. It adopts a fully passive safety system, which consists of a four-train independent passive safety injection system (PSIS) and a four-train independent passive residual heat removal system (PRHRS) using steam generators (SGs) and secondary system lines. The RCS NC phenomena in the SMART play significantly important

* Corresponding author. Innovative System Safety Research Division, Korea Atomic Energy Research Institute, 111, Daedeok-daero 989 Beon-gil, Yuseong-Gu, Daejeon, 34057, Republic of Korea.
E-mail address: hbae@kaeri.re.kr (H. Bae).

https://doi.org/10.1016/j.net.2021.08.023

Nomenclature

CLOF	complete loss of RCS flow
CMT	core makeup tank
CRA	control rod assembly
DBA	design basis accident
ECT	emergency cooldown tank
FLB	feedwater line break
LOCA	loss-of-coolant accident
NC	natural circulation
NSSS	nuclear steam supply system
PBL	pressure balance line
PRHRS	passive residual heat removal system
PSIS	passive safety injection system
PZR	pressurizer
RCP	reactor coolant system
RCS	reactor coolant system
RPV	reactor pressure vessel
SBLOCA	small break LOCA
SG	steam generator
SIL	safety injection line
SIT	safety injection tank
SMART	system-integrated modular advanced reactor
SMART-ITL	integral-effect test loop for SMART
SPNC	single-phase NC
TPNC	two-phase NC
VISTA	reduced-height integral test loop for SMART

roles in the RCS cooling performance during the specific design basis accidents (DBAs), such as the transients and loss-of-coolant accident (LOCA) situations. Single-phase NC is one of the major behaviors exhibited during the feedwater line break (FLB) and complete loss of RCS flow (CLOF) scenarios, in which the RCP is tripped and the secondary system comprising the SG secondary side and PRHRS removes the RCS decay heat. Both single- and two-phase NC in the RCS occur independently and sequentially in the DBA scenarios. In the early stage of the LOCA scenario, single-phase NC is the major behavior; subsequently, two-phase NC becomes the major phenomenon after the collapsed water level decreases below the RCP flow path. It is helpful to understand the NC phenomena practically expected to occur in the SMART through the analyses of robust-bounding tests using the SMART-ITL facility. Techniques used in SMART design need to be verified through various tests, including thermal-hydraulic validation tests. An integral-effect test loop for SMART (SMART-ITL) was designed to simulate the integral thermal-hydraulic behavior of SMART [7] and conduct full-height and multi-train loop NC tests. The objectives behind using the SMART-ITL are to investigate and understand the integral behavior of reactor systems and components, and the thermal-hydraulic phenomena occurring in the system during normal, abnormal, and emergency conditions. The integral-effect test data are also used to validate the related thermal-hydraulic models of the safety analysis code such as TASS/SMR-S [8], which is used for the performance and accident analysis of the SMART design. The TASS/SMR-S code was developed to analyze thermal-hydraulic phenomena under various transient and accident conditions.

In this study, NC tests were performed to investigate the NC characteristics for a reference plant under a change in the core power or RCS inventory. Three-step single-phase NC (SPNC) tests were carried out using the SMART-ITL under a constant core power and feedwater flow rate. Furthermore, a two-phase NC (TPNC) test was carried out with periodically repetitive discharging of the coolant inventory, to evaluate the two-phase natural circulation flow rate under a quasi-steady state with decreased inventory. The capability of the TASS/SMR-S code to simulate NC was validated using the test results.

2. SMART-ITL and TASS/SMR-S

2.1. SMART-ITL facility

The SMART-ITL is a thermal-hydraulic integral-effect test facility for SMART constructed at KAERI, and it is basically designed according to the volume scaling method to simulate various test scenarios as realistically as possible. The SMART-ITL facility involves the following characteristics: (a) 1/1-height, 1/49-vol, and full-pressure simulation of SMART; (b) geometrical similarity with SMART, including an integral arrangement of the primary systems; and (c) a maximum of 30% of the scaled nominal core power.

The scientific design of the SMART-ITL was accomplished from the viewpoints of both global and local scaling based on Ishii's three-level scaling methodology [9]. The major scaling parameters of the SMART-ITL facility are summarized in Table 1. A general arrangement of the SMART-ITL for the NC simulation is shown in Fig. 1 [10].

The fluid system of the SMART-ITL consists of a primary system, a secondary system, a PRHRS, a PSIS, a shutdown cooling system, a break simulating system, a break measuring system, and auxiliary systems. The primary system has an integral arrangement, except for the external installation of SGs, and it is composed of a reactor pressure vessel (RPV), four RCPs, four SGs, and primary connecting piping between the RPV and SGs. The secondary system of the SMART-ITL is simplified to be of the circulating loop type, and it is composed of a condenser, feedwater and steam lines, and related piping and valves. All the safety system features of the SMART plant are incorporated in the safety system of the SMART-ITL, which is composed of the PRHRS and PSIS. In the SMART-ITL test facility, over 1600 instrumentation devices have been installed to monitor and control the thermal-hydraulic behaviors during the simulation of various test scenarios. To allow for the simulation of high-pressure scenarios, the primary system has been designed to operate at pressures of up to 18 MPa.

2.2. TASS/SMR-S code

A five-equation code with a non-equilibrium two-phase flow model was developed using TASS/SMR-S V1.1 to improve the thermal-hydraulic prediction capability under the two-phase flow.

Table 1
Major scaling parameters of SMART-ITL.

Parameters	Value
Length	1/1
Area	1/49
Volume	1/49
Time scale	1/1
Velocity	1/1
Heat flux	1/1
Core power	1/49
Flow rate	1/49
Pump head	1/1
Pressure drop	1/1

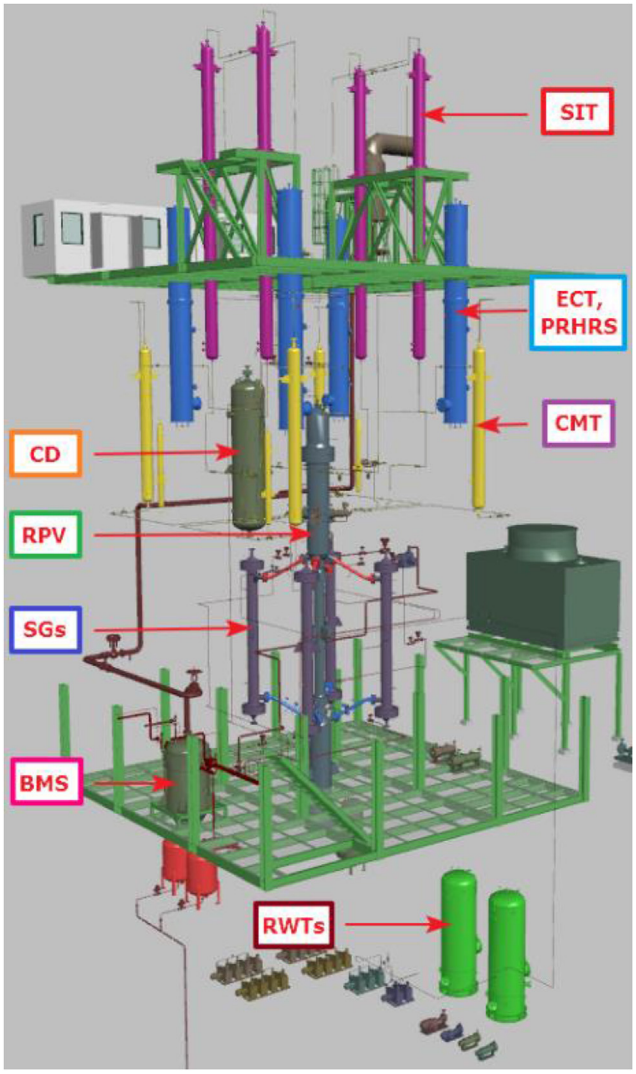

Fig. 1. General arrangement of SMART-ITL facility [10].

The five governing equations included the mixture mass, liquid mass, mixture momentum, mixture energy, and steam energy conservation equations with various thermal-hydraulic models. The transients are analyzed using the TASS/SMR-S code, which was developed to simulate the safety and performance related design basis events of the SMART plant [8].

Basically, the code models the plant as a set of nodes and paths to calculate the thermal-hydraulic behavior of the system, such as the core power, core heat flux, coolant temperature, coolant pressure, and flow rate.

The following functions are built into the TASS/SMR-S code to simulate the nuclear steam supply system (NSSS):

(1) Point kinetic neutronics
(2) Doppler and moderator reactivity feedback
(3) Control rod assembly (CRA) reactivity insertion
(4) Reactor core thermal-hydraulic characteristics
(5) Reactor coolant pressure change and mass transfer
(6) Pressurizer (PZR) behavior
(7) Non-condensable gas effect
(8) Thermal-hydraulics of once-through SGs
(9) Thermal-hydraulics of PRHRS

The TASS/SMR-S code is design code. It has been developed for the safety analysis of SMART, the standard design for which was approved in July 2012. The technical reports for the TASS/SMR-S code were submitted to the regulatory authority, which is the NSSC of Korea. The conservative analysis capability was verified through the review, but the regulatory authority required further evaluation with the experimental results of SMART-ITL, which is the integral test facility of SMART. Thus, the TASS/SMR-S code was evaluated with SMART-ITL test results, including the small break LOCA test, in the following project.

The nodalization for the SMART-ITL is depicted in Fig. 2. The RCSs, consisting of the secondary system from the feedwater control valves to the turbine trip valves, safety injection tanks (SITs), core makeup tanks (CMTs), and the PRHRS, are modeled with nodes and paths. The nodalization is basically consistent with the validation of the LOCA test [11,12].

The RCS consists of the heater for the core simulation, upper plenum, RCP, SG primary side, downcomer, core bottom region, and PZR. The heater rods are modeled with ten nodes, while the core bypass region is modeled with three nodes. The PZR is modeled with ten nodes to predict complex behavior during the early stages of a violently transient phenomenon, such as LOCA.

The secondary system consists of the feedwater isolation valve, feedwater pipe, SG secondary side, steam pipe, and steam pipe isolation valve. The four SGs are modeled with 12 nodes each. The feedwater is set as a boundary condition using the feedwater model of the TASS/SMR-S code, while the steam lines are only modeled up to the turbine control valve.

The PRHRS is connected downstream of the feedwater isolation valve and upstream of the steam isolation valve. The PRHRS heat exchangers are modeled with four nodes arranged in the axial direction, and the emergency cooldown tank (ECT) is modeled with 14 nodes to simulate the overall circulation in the ECT.

The PSIS is connected at the RCP discharge side of the RPV. The CMT and SIT of the PSIS are modeled with five nodes for each component. The pressure balance line (PBL) and safety injection line (SIL) are modeled with eight and four nodes, respectively.

3. NC tests using SMART-ITL facility

3.1. Conditions and procedures for NC tests

Three SPNC tests using SMART-ITL were carried out through a four-step test procedure: startup operation, heat-up operation, steady-state operation, and SPNC test. After the steady-state operation at 15% core power was attained, the NC test commenced as soon as the RCPs stopped. Three NC tests were sequentially conducted during the three-step core power reduction at 15%, 10%, and 5%. The NC in the reference plant design is estimated at under 20% of the rated flow rate. In the SMART-ITL simulation, 15% of the scaled full power was selected as the upper limit of NC to protect the core heater. On the other hand, the decay heat was simulated by an ANS-73 curve under an accident accompanied by the core trip. The power fraction of the ANS-73 curve suddenly decreased to 5% within approximately 50 s and it required 40,000 s to decrease below 1% of the full power. As it is difficult for the feedwater flow rate to be maintained at under 5% of the rated flow rate in the SMART-ITL, 5% was selected as the lower limit of the NC tests. The core power fraction denotes the ratio for the scaled full power. The reference nuclear power plant was the SMART, which has a capacity of 365 MWth. The SMART-ITL was scaled down to 1/49 applied by the volume scale law with the same height. In other words, the scaled full power was approximately 7.5 MWth. The feedwater flow rates corresponded to the scaled ratio of 15%, 10%, and 5%, respectively. In each test, the feedwater flow rates were adjusted by the

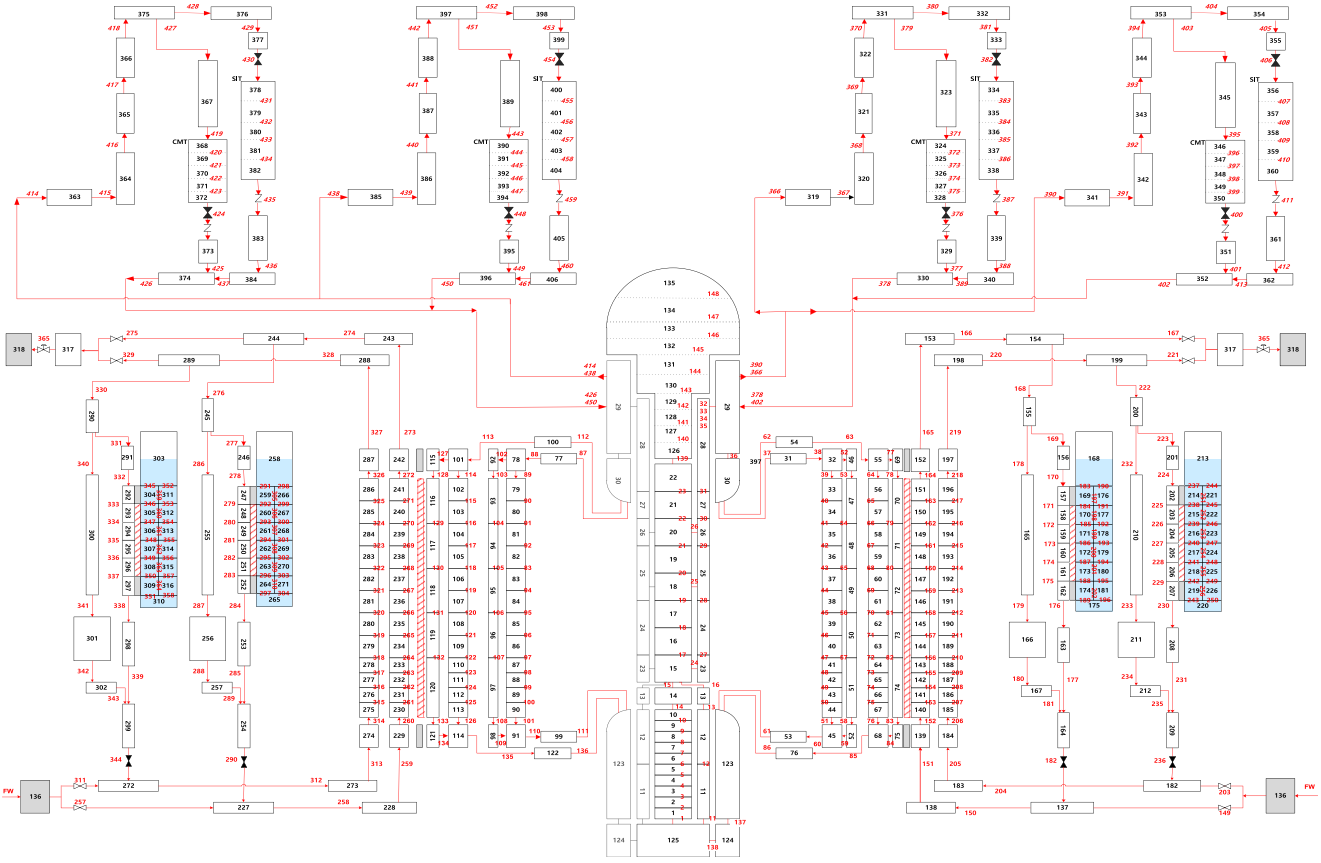

Fig. 2. Nodalization for the SMART-ITL facility.

corresponding ratio.

STDY-15P represents a steady-state test with the RCP working under an initial condition for the SPNC test listed in Table 2. The target values in Table 2 denote the nominal operation condition to apply the scale ratio of the SMART-ITL. Most of the measured values are satisfied with the target ones within 5% difference, except for the core power, RCS flow rate, and feedwater pressure. The measured core power was 15.94% higher than the target because the core power in the test should include the heat loss of the structures. The target core value denotes the fraction of the scaled full power. For example, 1.117 MW corresponds to 15% of the scaled full power of 7.5 MW. The facility suffers from heat loss, and the core power should, therefore, be sufficiently high to compensate for the heat loss and the secondary heat removal in order to satisfy approximately 1.117 MW. In the SMART-ITL facility, heat loss is considered by adding a heat loss of 163 kW to the heat removal at the SG secondary side of 1132 kW. Therefore, the core power is 1295 kW with the heat loss of 163 kW, and the heat removal at the

Table 2
Results from test and calculation for SPNC.

Value	Unit	STDY-15P			SPNC-15P		SPNC-10P		SPNC-5P	
		Target value	Measured	Calculated/ Measured (%)	Measured	Calculated/ Measured (%)	Measured	Calculated/ Measured (%)	Measured	Calculated/ Measured (%)
Core Power	kW	1117	1294.815	100.01	1294.641	99.99	849.948	100.00	548.29	100.00
PZR Heater	kW		31.49		31.05		24.84		25.48	
RCS Total Mass Flow Rate	kg/s	7.674	8.6915	100.01	6.0598	103.25	5.1574	100.91	4.4996	94.57
PZR Pressure	MPa	15	15.03	99.93	15.19	99.61	15	99.87	15.03	99.27
Core Inlet Fluid Temperature	°C	295.5	296.2	99.97	290.3	100.20	292.85	100.39	302.09	98.28
Core Outlet Fluid Temperature	°C	320.9	322.02	99.98	327.24	99.83	321.68	100.23	322.81	98.93
PZR Temperature	°C	342.13	341.71	100.18	342.54	100.09	341.58	100.21	341.79	100.11
Total Feedwater Flow Rate	kg/s	0.584	0.584	99.99	0.5754	100.30	0.3645	100.00	0.2086	100.00
Feedwater Pressure	MPa	6.71	5.68	100.00	5.6771	100.07	5.6524	99.82	5.667	99.77
Main Steam Pressure	MPa	5.62	5.61	100.00	5.61	100.00	5.61	100.00	5.64	100.00
Feedwater Temperature	°C	230	230.13	99.99	230.18	100.00	230.18	100.00	226.01	100.00
Main Steam Temperature	°C	302.3	315.05	99.99	319.42	99.23	313.14	101.93	309.99	102.70

steam generator is approximately 1132 kW. To satisfy the temperatures of the core and SG primary side under this special situation, the given RCS flow rate should be higher than the target. It was revealed that the heat balance between the RCS and secondary system was well maintained, which proves that the heat transfer rate on the secondary side of the SG was similar to the target core power. The target feedwater pressure refers to the pressure for the rated flow rate. The actual feedwater pressure could not be attained with the target value of approximately 15% of the rated flow rate, because it is proportional to the feedwater flow rate.

The test procedure of the SPNC is listed in Table 3. Individual tests should involve the maintenance of a quasi-steady operation for a certain duration. Some variables such as the core heater power, feedwater temperature, and flow rate should be precisely controlled at a constant temperature and pressure of the RCS until all the conditions attain steady-state trends. As a result, once the RCS NC flow rate that satisfies the heat balance between the RCS and secondary system is reached, the state is maintained for a certain period of time. The test was continued by reducing the core power in steps of 5%, with a corresponding reduction in the feedwater flow rate. SPNC-15P refers to a quasi-state SPNC test result for 15% core power after the RCP trip. Both SPNC-10P and SPNC-5P refer to the results of quasi-state SPNC tests for 10% and 5% core power, respectively, with corresponding reductions in the feedwater flow rate.

A major issue in the TPNC test was the need to investigate various thermal-hydraulic behaviors while decreasing the RCS inventory and under a robust boundary condition, such as a constant core heat power, to maintain the decay heat level and feedwater flow rate. The TPNC test proceeded with the special SBLOCA scenario that occurred in a specific nozzle mounted in the lower part of the RPV. A break and standby were simulated periodically. The discharge of the reactor coolant in the TPNC was used as a specific method to investigate the NC characteristics according to the change in the reactor coolant inventory. Thus, to evaluate the two-phase natural circulation flow rate under a quasi-steady state with the decreased inventory, the process of releasing the coolant and maintaining the NC was repeated periodically. The discharging valve simulated the SBLOCA. The break nozzle size was scaled down to 1/49 of the 2-inch break SBLOCA of the reference plant, SMART. TPNC was carried out for 5% core power, the minimum fraction required to maintain the steady-state condition. Simultaneously, mass inventory was discharged repeatedly in a periodic sequence. The TPNC test was conducted sequentially after the completion of the last SPNC test with 5% core power (550 kW, SPNC-5P); it was initialized by opening the discharge valve located at the lower downcomer (Fig. 3). The discharge valve was fully opened for 20 s, and the main thermal-hydraulic parameters were subsequently investigated for 5 min, with the valve closed. The process of opening and closing the valve was periodically repeated, as shown in Table 4. A detailed logical explanation of the TPNC test results, in addition to the TASS/SMR-S analysis, is presented in Sections 3.3 and 4.2.

3.2. SPNC tests results

Three SPNC tests were performed with the SMART-ITL facility while maintaining four types of quasi-steady-state conditions. Considering 15% core power with RCP operation as the initial condition, the SPNC tests were sequentially performed at 15%, 10%, and 5% core power without RCP operation, as mentioned in Section 3.1. Figs. 4–7 show the test results, such as the core power, RCS flow rate, feedwater flow rate, and heat transfer rate. The SPNC results of the tests are listed in Table 2. After the RCP trip, the core power and feedwater flow rate were adjusted sequentially, and the SPNC flow rate of the RCS was generated appropriately. The heat transfer rates of the SGs were in good agreement with each other, suggesting that all the major parameters were well controlled and the SPNC flow rate remained stable for a certain duration.

3.3. TPNC tests results

The TPNC test followed the SPNC tests and was initialized by opening the discharge valve located at the lower downcomer (Fig. 3) from the SPNC under the 5% core power (SPNC−5P) condition. The discharge valve was fully opened for 20 s, and the main thermal-hydraulic parameters were then investigated for 5 min with the valve closed. Fig. 8 shows the accumulated break flow. The process of opening and closing the valve was periodically repeated, as shown in Table 4.

Figs. 9–13 show the results of the TPNC tests and TASS/SMR-S calculations at 5% power (550 kW), including the core power, RCS pressure, fluid temperatures and saturated temperatures at the core inlet and outlet, collapsed water level in RPV, and RCS flow rate [4]. As the TPNC test was initialized by opening the discharge valve under the steady-state condition with 5% core power, the core power was maintained at 5% in the tests, as shown in Fig. 9; Fig. 10 presents the RCS pressure. Once the discharge valve was opened,

Table 3
Procedures for SPNC test.

Event	Time	Setpoint	Remark
Initial Condition (15%)	–	Core power: 1295 kW RCS flow rate: 8.679 kg/s FW flow rate: 0.577 kg/s (Active operation)	Table 2
Steady State	–	~ 801 Seconds	>600 s STDY-15P
RCP trip			Manual Stop
FW Flow Rate Control		FW: 0.575 kg/s (Natural Circulation)	FW pump: manual control, FW temp. and pressure
Quasi Steady State	>10 min	RCS: 6.065 kg/s	SPNC-15P
Core Power 10%		Core power: 850.4 kW	Manual control
FW Flow Rate Control		FW: 0.363 kg/s	FW pump: manual control, FW temp. and pressure
Quasi Steady State	>10 min	RCS flow rate: 5.154 kg/s (Natural Circulation)	SPNC-10P
Core Power 5%		Core power: 550.2 kW	Manual control
FW Flow Rate Control		FW: 0.212 kg/s	FW pump: manual control, FW temp. and pressure
Quasi Steady State	>10 min	RCS: 4.488 kg/s (Natural Circulation)	SPNC-5P
Test End			

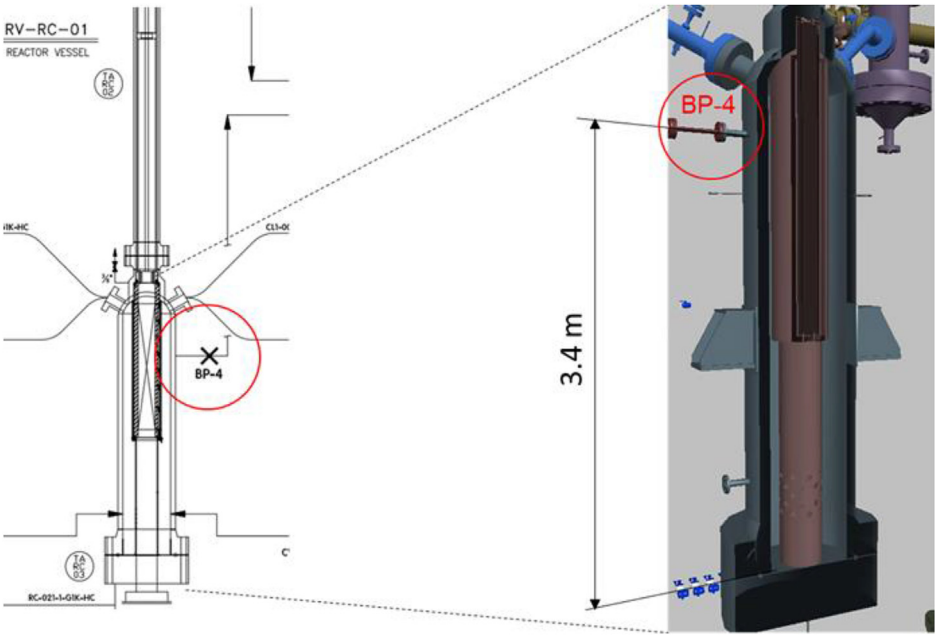

Fig. 3. Location of discharge for TPNC test.

Table 4
Sequence of two phase natural circulation.

No.	Event	Set Point or Time	Operation Condition	Remark
1	Initial Condition		- Core power: 550 kW - RCS flow: 4.488 kg/s - FW flow: 0.208 kg/s	Natural Circulation in RCS
2	Steady State		634 s	>600 s
3	Discharge of Reactor Coolant	20 s		
4	RCS condition - If it satisfies criteria, 5 - If not, 7	Surface temperature of core heater rod Flowrate in cold leg Water level in vessel		<600 °C Existence of flow >4 m
5	Collection of TH data	>5 min		
6	Repeat discharge process (3 through 5)		35 times	
7	Termination			

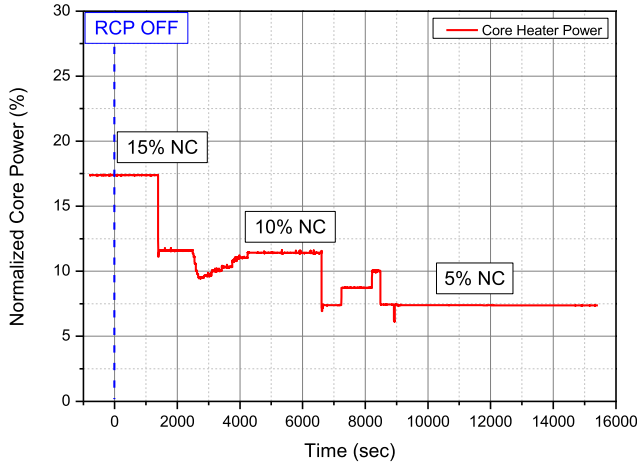

Fig. 4. Core power for SPNC.

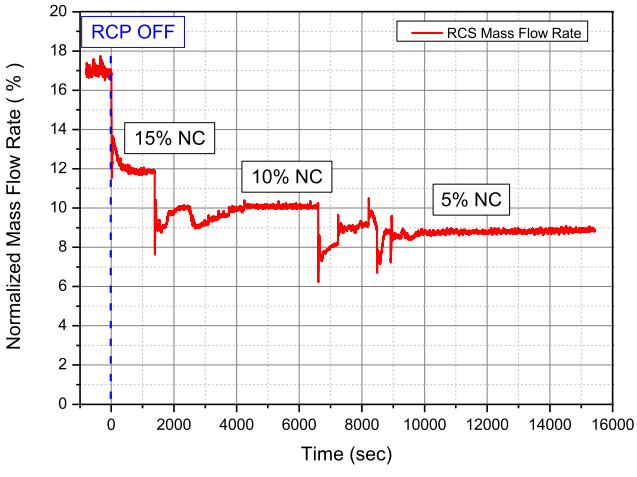

Fig. 5. RCS flow rate for SPNC.

the RCS pressure gradually decreased, while maintaining a sub-cooled condition. From approximately 2000 s, the pressure was maintained at approximately 12 MPa because the RCS thermal-hydraulic condition reached saturation, which was also evident from the trends of fluid temperatures in the core (Fig. 11). At approximately 6000 s, the pressure gradually increased because of

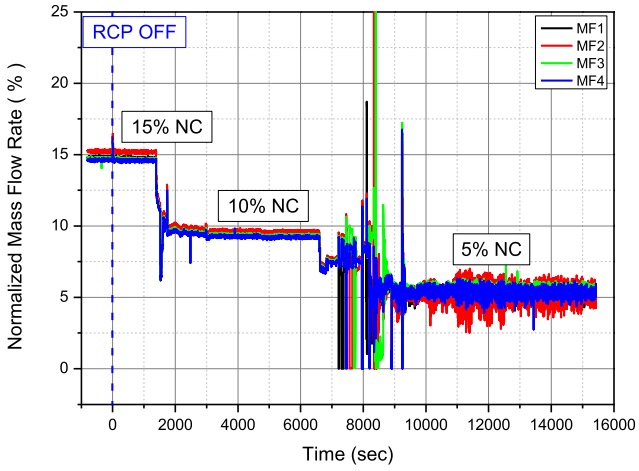

Fig. 6. Feedwater flow rate of secondary system for SPNC.

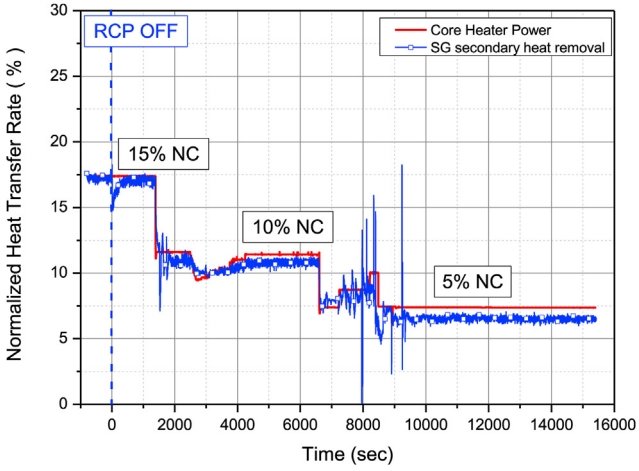

Fig. 7. Heat transfer rate between RCS and secondary system for SPNC.

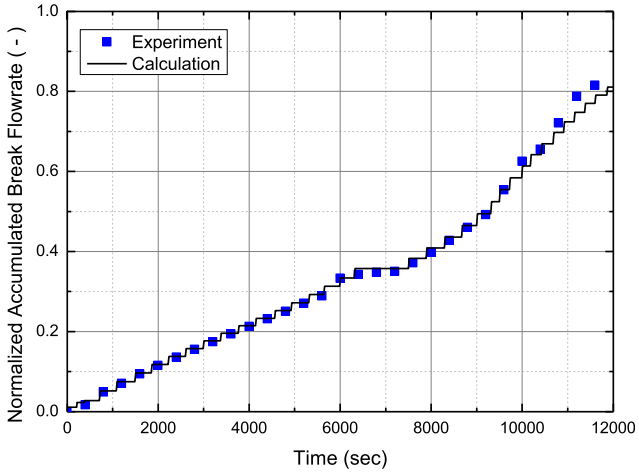

Fig. 8. Accumulated break flowrate in TPNC calculation of TASS/SMR-S compared with test.

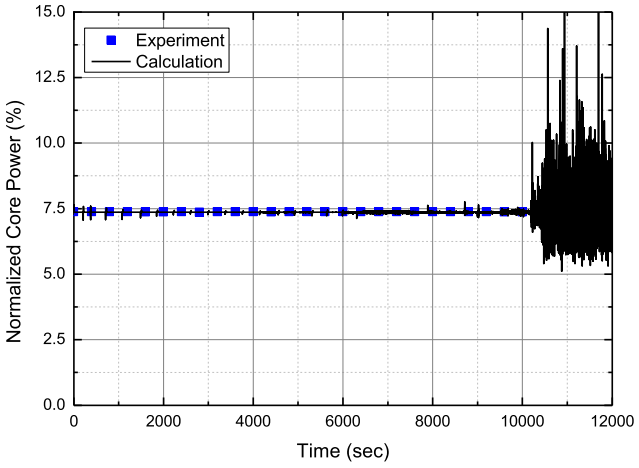

Fig. 9. Core power in TPNC calculation of TASS/SMR-S compared with test.

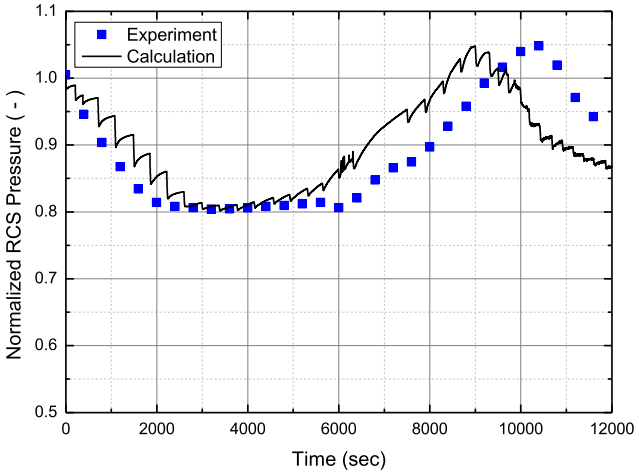

Fig. 10. RCS pressure in TPNC calculation of TASS/SMR-S compared with test.

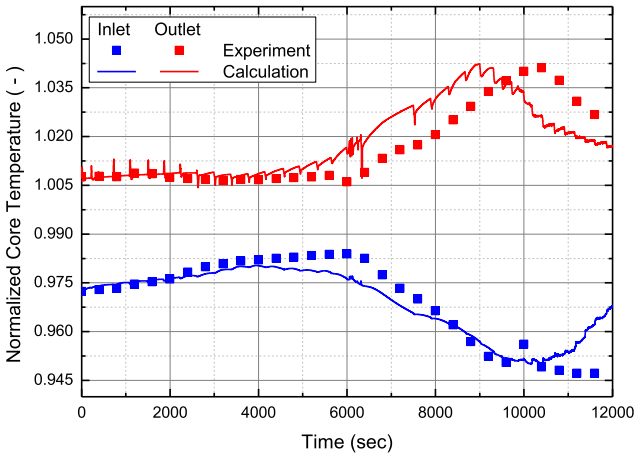

Fig. 11. Core temperatures in TPNC calculation of TASS/SMR-S compared with test.

the increased boiling, as evidenced by Fig. 12, which represents the continuous decrease of the collapsed water level in the RPV. The pressure reached the maximum value at approximately 10,000 s, and it then decreased with the temperature of the hot-leg pipe. The RCS pressure distribution can be classified into four states: the sub-cooling state up to 2000 s, the saturation state up to 6000 s, the boiling state up to 10,000 s, and the condensation state beyond

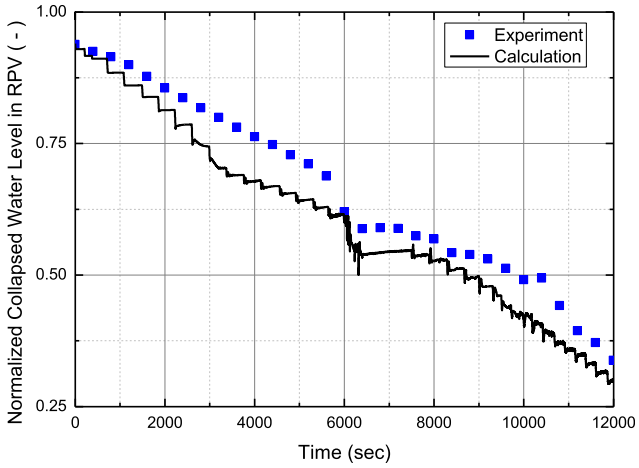

Fig. 12. Collapsed water level in RPV in TPNC calculation of TASS/SMR-S compared with test.

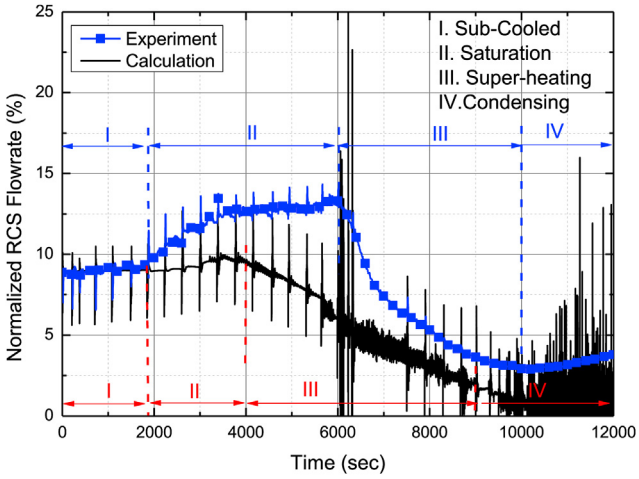

Fig. 13. RCS flowrate in TPNC calculation of TASS/SMR-S compared with test.

10,000 s. Fig. 13 shows the RCS flow rate. The TPNC flow rate for the test exhibits an unstable behavior; it was reproduced by a method similar to that used for the SPNC, which was obtained by dividing the core power with the core inlet/outlet enthalpy difference, in order to additionally account for the void fraction and quality [13]. The evaluated flow rate shows a reasonable behavior, especially for the two-phase flow. The NC flow rate was related to the behavior of pressure and temperature. The temperature difference between the inlet and the outlet of the core decreased (as shown in Fig. 11) until the RCS pressure reached saturation at approximately 2000 s. The RCS flow generally maintained a constant NC flow rate in the single-phase state. While the pressure remained constant in the saturated state from 2000 to 6000 s, the temperature difference between the core inlet and the outlet also remained constant. Conversely, the RCS NC flow rate gradually increased and approached the two-phase state under the saturation condition. In the initial period from 6000 to 10,000 s, the temperature at the core outlet increased when the pressure of the RCS increased and the temperature at the core inlet decreased; the NC flow tended to decrease dramatically. After 10,000 s, the RCS flow rate exhibited a gradual decrease, followed by a constant value on average at approximately 11,000 s; the RCS pressure also decreased. It can be concluded that this was likely caused by the loss of potential energy to maintain the NC as the coolant inventory decreased and the reduced evaporation within the core.

4. Analysis using TASS/SMR-S code

4.1. Validation results against SPNC tests

The TASS/SMR-S codes were calculated separately for the individual cases, even though the SPNC tests were carried out continuously [14]. It was convenient to control the core power, feedwater flow rate, and heat loss coefficient of the heat structures for each case, and individual calculation results were used as the initial condition for the subsequent calculations.

In the analysis, the core power and feedwater flow rate were obtained from boundary conditions based on the test data. The options employed to calculate the single-phase state, including the initial conditions and the quasi-steady state for the SPNC, were as follows:

(1) All nodes apply homogeneous and equilibrium options except for the pressurizer, CMT, and SIT nodes, which apply a non-homogeneous option.
(2) All paths do not apply a drift-flux option.
(3) As the initial condition, the ambient heat loss from the RCS for the steady state was assumed to be 163 kW. This value was calculated based on the steady-state test data.

The validation analysis for the SPNC tests was performed independently, and individual results were used as the initial conditions for the following calculations. To attain a quasi-steady-state condition for each core power, transient mode calculations were performed using the previous step results as the initial conditions. The SPNC-15P analysis was commenced with the RCP trip using the previous results, i.e., STDY-15P, as the initial condition. The same procedure was applied for SPNC-10P and SPNC-5P, with an additional control to appropriately reduce the feedwater flow rate. The SPNC results of the calculations are listed in Table 2. Overall, the results calculated using TASS/SMR-S confirm them to be reasonably accurate predictions in comparison with the measured values; the temperatures of the reactor core and SG were predicted well, within an accuracy of 1%. The capability of TASS/SMR-S was evaluated via the results obtained using the SMART-ITL from the three SPNC tests.

Achieving heat balance is considerably important to maintain the steady-state condition during SPNC tests. The heat balance between the core power and the secondary heat removal is presented in Fig. 14, which shows good agreement in terms of the heat balance between the SPNC tests and the TASS/SMR-S calculations. At all stages of calculation, the core power was provided as a fraction of the secondary heat removal from the SGs, and the heat loss of the RCS estimated from the tests was provided as the input value for individual calculations. The heat loss of 163 kW was estimated by subtracting the heat removal on the SG secondary side, which was calculated as 1132 kW during the STDY-15P, from the actual core power. Therefore, 163 kW is divided by the actual core power, 1295 kW; thus, the heat loss ratio based on the secondary heat transfer rate could be estimated as 12.6%. The most significant heat loss occurs in the cold legs, which refer to the pipes connecting the SG primary side with the lower downcomer. There exist a few methods to reduce heat loss, such as heat loss compensation with heat tracing, increasing core power or the RCS flow rate, and insulating pipes and components. Heat tracing is a highly useful method under the steady-state condition. However, simulating it under the transient condition is considerably difficult. The calculation results reveal that the amount of secondary heat

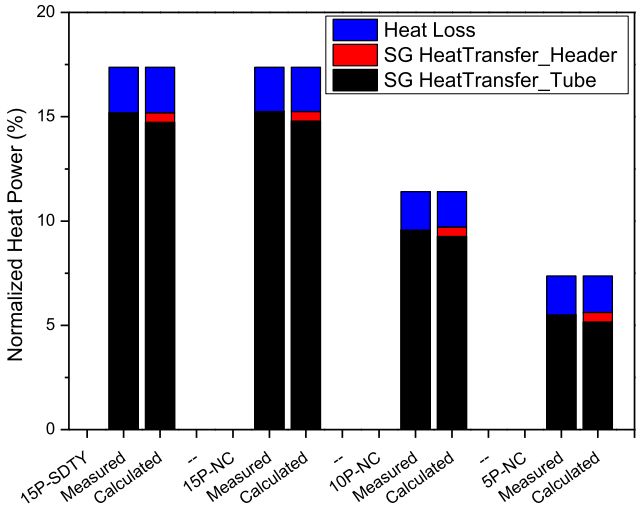

Fig. 14. Heat balance with test and calculation.

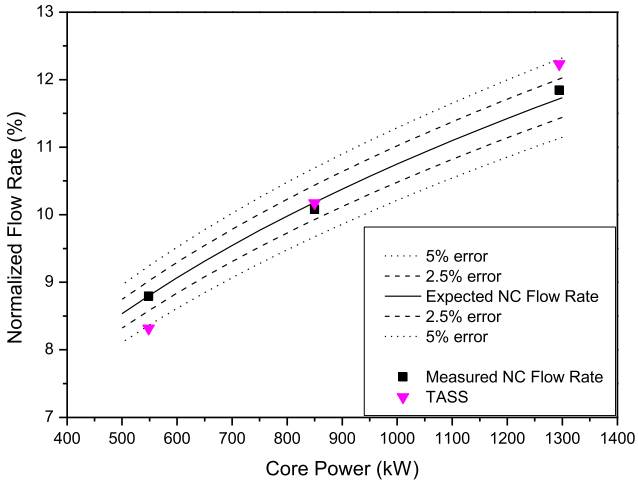

Fig. 15. Natural circulation flow rate in the test and calculation.

removal in the SG includes a sum of the heat transfer rate in the tubes and their headers.

4.2. Validation results against TPNC tests

As mentioned in Section 4.1, the TPNC test was initialized by opening the discharge valve located at the lower downcomer after the SPNC test involving 5% core power. The break was modeled at node 123 with an inner diameter of 7.26 mm. Fig. 8 shows the accumulated break flow. Good agreement between the experimental measurements and the calculation results was noted; this confirms that the break was modeled well as a boundary condition. Other boundary conditions, i.e., the core power, heat loss, and feedwater flow rate, were maintained as the initial conditions throughout the calculation. To model the two-phase flow accurately, other validation models such as the drift-flux model, heterogeneous option, and non-equilibrium option, which are basically equivalent to the modeling in the validation calculation of SBLOCA, were applied as follows [11,12]:

(1) A non-equilibrium option was applied to every node of the core, PZR, SG, CMT, and SIT, which occurred as a result of the heat transfer during the phase change in the transient condition.
(2) A heterogeneous option was additionally applied to the upper regions of the upper plenum (Nodes 20, 21, and 22), where the two-phase flow was expected to be dominant.
(3) A drift-flux option was applied to every path of the RCS, except for UGS hall, UGS upper part, RCP, PZR, and bypass nodes of the SG and core.
(4) Break flow rate was determined using the modified Henry-Fauske model.

5. Results and discussion

The SPNC flow rates for various core power values, as obtained from the tests, calculations, and correlation, are shown in Fig. 15. First, the RCS flow rate for the tests was reproduced by a reverse calculation for the heat balance method of the RCS using the core power and temperatures at the inlet and outlet to confirm the measured SPNC flow rate. The reverse estimation provides reasonable results, as presented in this paper. Second, the calculation results were under-predicted at lower power values and over-predicted at higher power values, in comparison to the test results. Third, the results from the test and calculations were compared to a well-known correlation, which is expressed in Equation (1) [15], for the SPNC related to the core power. In the original correlation equation, C is a coefficient consisting of the cross-sectional area (A) in the test section, the pressure loss coefficient (K), the center distance (L) between the heat source and the heat sink, and the volumetric thermal expansion coefficient (β). However, the shape of the piping in SMART-ITL can be highly diverse; therefore, the definitions for the cross-sectional area and pressure loss coefficient are quite complex. In this case, the coefficient C can be defined as a constant through tests. The constant in the NC flow correlation for SMART-ITL, obtained through the previous test, is 0.548 [16]. A comparison of the core power used as the input in the TASS/SMR-S calculation and the correlation results, as shown in Fig. 15, reveals that it is distributed approximately 5% higher than the correlation results at 15% core power and approximately 5% lower at 5% core power. The calculated NC flow rate is over- or under-predicted within ±5%, although the calculated flow rate according to the decrease in the core power was under-predicted in the experimental results. In general, the NC flow rate is a function of the flow resistance, which is determined by the pressure loss in system. 64/Re is implemented for the laminar flow region as a pressure loss model in the TASS/SMR-S code. Based on the test results, it is necessary to improve the pressure loss model for laminar flows. Evaluations for the laminar and turbulent flows in the NC tests are presented in the Appendix.

$$\dot{m} = CQ^{1/3} \tag{1}$$

$$C = \left|\frac{2A^2\beta g\rho_l^2\Delta L}{C_v K_1}\right|^{1/3} \tag{2}$$

Figs. 9–13 present comparisons of the main thermal-hydraulic parameters of the results obtained via the TPNC test and the calculated results from TASS/SMR-S, including the core power, RCS pressure, collapsed water level in the RPV, core inlet and outlet temperatures, and RCS flow rate.

As the TPNC test was initialized by opening the discharge valve under the steady-state condition with constant core power (550 kW), the core power was maintained at 5% of the full power, as in the experiment depicted in Fig. 9.

Fig. 10 presents the RCS pressure. The TASS/SMR-S calculation

was highly congruent with the experimental results, but an increase in pressure occurred at approximately 4000 s. This is approximately 2000 s earlier than that in the test, where the pressure increases at 6000 s. This implies that TASS/SMR-S predicts a greater amount of boiling than that in the test. This phenomenon is also illustrated in Fig. 12, where the calculated collapsed water level is lower than that from the test beyond 4000 s. The void fraction was not measured directly; it is generally calculated based on the collapsed level. Fig. 12 compares the collapsed levels between the tests and the calculation. The collapsed level can be used as a representative parameter for the boiling phenomenon.

Fig. 11 shows the predictions of the core inlet and outlet temperatures from the TASS/SMR-S calculation; these follow the experimental results in general. The temperature trend at the core outlet also exhibits an earlier increase, which is due to the same reason as the trend of the RCS pressure.

Fig. 13 shows the RCS flow rate with large periodical oscillations whenever the break valve opens or closes. The overestimation of boiling in TASS/SMR-S, which is the main cause of all the differences between the calculations and tests, is also presented in other validations of TASS/SMR-S [17]. The thermal-hydraulic condition of the RCS in the TPNC test can be classified into four states, as mentioned in Sec. 3.3: the sub-cooling state up to 2000 s, the saturation state up to 6000 s, the boiling state up to 10,000 s, and the condensation state beyond 10,000 s. However, the results of TASS/SMR-S indicate the sub-cooling state up to 2000 s, the saturation state up to 4000 s, the boiling state up to 9000 s, and the condensation state beyond 9000 s. For the sub-cooled state during the earlier stages of the TPNC test, SPNC is the main flow behavior observed. TPNC begins to appear after the saturation state. In the boiling state, TPNC is the dominant phenomenon. TASS/SMR-S has been developed as safety analysis code for SMART. It features conservatism for the models and input variables. This conservatism results in the overestimation of the boiling calculations from TASS/SMR-S. Overall, the calculated NC flow rate is predicted to be lower than the test results, although it exhibits a similar trend. After 4000 s, the NC flow rate tends to be proportional to the decrease in the coolant inventory. Considering the time difference due to the overestimation of boiling in TASS/SMR-S, major thermal-hydraulic parameters such as the pressure, temperature, and TPNC flow rate are highly consistent with the test results.

6. Conclusion

In this study, three SPNC tests and one TPNC test with periodically repetitive reactor coolant discharges were carried out using the SMART-ITL facility, under individually constant core power values and feedwater flow rates. Most measured values for the SPNC tests were reasonably in agreement with the target values, and scenarios involving single-phase, saturated, and two-phase states in the TPNC test were well investigated.

The TASS/SMR-S code was validated using the results from the SPNC and TPNC tests, performed using the SMART-ITL facility. The validation against the SPNC tests revealed that the overall thermal-hydraulic behaviors of the primary and secondary systems were accurately predicted. The NC in the RCS was also predicted reasonably well by the code. Furthermore, the validation against the TPNC test revealed that the overall thermal-hydraulic behaviors, such as the RCS pressure, core temperature, and NC flow rate, were predicted reasonably close to the desired values.

However, the TASS/SMR-S code exaggerated the level of boiling; moreover, it predicted earlier increments in the RCS pressure and core temperature and an earlier decrease in the NC flow rate, as compared to the actual test results. These deficiencies indicate that the TASS/SMR-S code estimates the boiling phenomenon under the two-phase condition conservatively. Therefore, it can be concluded that the TASS/SMR-S code exhibits somewhat conservative but comparable results in terms of the overall thermal-hydraulic trends.

Declaration of competing interest

The authors declare that they have no known competing financial interests or personal relationships that could have appeared to influence the work reported in this paper.

Acknowledgments

This work was supported by the SMART Standard Design Change Approval Project funded by KAERI, South Korea, KHNP, South Korea, and K.A. CARE, Kingdom of Saudi-Arabia.

Appendix

Using the parameters measured under the 15% SPNC test condition, the Reynolds number is approximately 375; this reveals that the NC flow is laminar rather than a fully developed turbulent flow. It is expected that the lower the simulated core power, the lower the predicted flow rate. For example, the Reynolds number is calculated as follows:

- Parameters: 15 MPa, 300 °C, 1.9185 kg/s (per SG cold leg, total flow rate: 7.674kg/s), 0.11 m (inner diameter for a single cold leg).
- The measured flow rate is the summation of the values from the four flow meters on the individual cold legs.
- Re = 375 (i.e., very low Reynolds number)

References

[1] IAEA, Natural Circulation Phenomena and Modelling of Advanced Water Cooled Reactors, IAEA-TECDOC-1677, Vienna, 2012.
[2] F. D'Auria, M. Frogheri, Use of a natural circulation map for assessing PWR performance, Nucl. Eng. Des. 215 (2002) 111–126.
[3] H.S. Park, K.Y. Choi, S. Cho, S.J. Yi, Experimental investigations on the heat transfer characteristics in a natural circulation loop for an integral type reactor, Int. Commun. Heat Mass Tran. 38 (2011) 1232–1238.
[4] M.R. Gartia, P.K. Vijayan, D.S. Pilkhwal, A generalized flow correlation for two-phase natural circulation loops, Nucl. Eng. Des. 236 (2006) 1800–1809.
[5] K.K. Kim, W. Lee, S. Choi, H.R. Kim, J. Ha, SMART: the first licensed advanced integral reactor, J. Energy Power Eng. 8 (2014) 94–102.
[6] IAEA, Advances in Small Modular Reactor Technology Developments, Vienna, 2020.
[7] H.S. Park, S.J. Yi, C.H. Song, SMR accident simulation in experimental test loop, Nucl. Eng. Int. Nov. (2013) 12–15.
[8] S.W. Lee, Development of Non-equilibrium and Non-homogeneous Model of TASS/SMR-S, KAERI/TR-6278/2015, KAERI, 2015.
[9] M. Ishii, I. Kataoka, Similarity Analysis and Scaling Criteria for LWRs under Single-phase and Two-phase Natural Circulation, NUREG/CR-3267, ANL-83-32, Argonne National Laboratory, 1983.
[10] H. Bae, S.U. Ryu, B.G. Jeon, J.H. Yang, E. Yun, Y.G. Bang, S.J. Yi, H.S. Park, Core makeup tank injection characteristics during different test scenarios using SMART-ITL facility, Ann. Nucl. Energy 126 (2019) 10–19.
[11] Y.J. Chung, B.G. Jeon, K.H. Bae, H.S. Park, Validation with the MARS and TASS/SMR codes based on experimental results of a pressurizer safety valve line break at the SMART-ITL facility, Ann. Nucl. Energy 141 (2020) 1–7.

[12] S.W. Lim, TASS/SMR-S Code Evaluation Using Integral Effect Test Results, KAERI/TR-6280/2015, KAERI, 2015.
[13] B.G. Jeon, E.K. Yun, H. Bae, J.H. Yang, S.U. Ryu, Y.G. Bang, S.J. Yi, H.S. Park, Two-phase Natural Circulation Test with SMART-ITL, 2021 submitted to Nuclear Engineering and Technology.
[14] H. Bae, J.H. Chun, Y.J. Chung, H.S. Park, TASS/SMR-S analysis on a single-phase natural circulation phenomenon in SMART-ITL during 3-different operating conditions, in: Transactions of the Korean Nuclear Society Spring Meeting, 2020. July 9-10, Jeju, Korea.
[15] R.B. Duffey, J.P. Sursock, Natural circulation phenomena relevant to small breaks and transients, Nucl. Eng. Des. 102 (1987) 115–128.
[16] E.K. Yun, Analysis on the Heat Balance and Natural Circulation during Integral Effect Tests Using SMART-ITL, KAERI/TR-6871/2017, KAERI, 2017.
[17] Y.J. Chung, TASS/SMR-S Code Evaluation Using Separate Effect Test Results, KAERI/TR-6279/2015, KAERI, 2015.